

Design, Synthesis, and Biological Evaluation of Hydroquinone Derivatives of 17-Amino-17-demethoxygeldanamycin as Potent, Water-Soluble Inhibitors of Hsp90

Jie Ge,[†] Emmanuel Normant,[†] James R. Porter,^{*,†} Janid A. Ali, Marlene S. Dembski, Yun Gao, Asimina T. Georges, Louis Grenier, Roger H. Pak, Jon Patterson, Jens R. Sydor, Thomas T. Tibbitts, Jeffrey K. Tong, Julian Adams, and Vito J. Palombella

Infinity Pharmaceuticals, Inc., 780 Memorial Drive, Cambridge, Massachusetts 02139

Received March 17, 2006

17-Allylamino-17-demethoxygeldanamycin (17-AAG)¹ is a semisynthetic inhibitor of the 90 kDa heat shock protein (Hsp90) currently in clinical trials for the treatment of cancer. However, 17-AAG faces challenging formulation issues due to its poor solubility. Here we report the synthesis and evaluation of a highly soluble hydroquinone hydrochloride derivative of 17-AAG, **1a** (IPI-504), and several of the physiological metabolites. These compounds show comparable binding affinity to human Hsp90 and its endoplasmic reticulum (ER) homologue, the 94 kDa glucose regulated protein (Grp94). Furthermore, the compounds inhibit the growth of the human cancer cell lines SKBR3 and SKOV3, which overexpress Hsp90 client protein Her2, and cause down-regulation of Her2 as well as induction of Hsp70 consistent with Hsp90 inhibition. There is a clear correlation between the measured binding affinity of the compounds and their cellular activities. Upon the basis of its potent activity against Hsp90 and a significant improvement in solubility, **1a** is currently under evaluation in Phase I clinical trials for cancer.

Introduction

Hsp90⁶⁸ is increasingly recognized as an important target for molecular cancer therapy due to its role in regulating key proteins in cell growth, survival, and differentiation pathways.^{1–5} Together with co-chaperone proteins (e.g., Hsp70, Hip, Hop, Hsp40, Cdc37, p23), Hsp90 assists the folding, maturation, stability, and trafficking of a specific group of proteins called client proteins.⁶ Hsp90 is ubiquitously expressed and is one of the most abundant proteins inside the cell, constituting up to ~2% of total protein.⁷ Frequent overexpression of Hsp90 in solid and hematologic tumors suggests a role for the chaperone in oncogenesis.^{8–16} Many of Hsp90 client proteins, including steroid hormone receptors, signaling kinases, transcription factors, and telomerase, appear to be involved in all the hallmarks of cancer.³ Thus inhibition of Hsp90 is proposed to simultaneously disrupt multiple oncogenic signaling pathways, thereby preventing drug resistance. Moreover, a number of Hsp90 clients in the kinase family contain or acquire mutations that lead to oncogenic activation or resistance to drug inhibition. These same mutations often render the client proteins more sensitive to Hsp90 inhibitors compared with their wild-type counterparts, with examples including imatinib-resistant (T315I and E255K) mutants of BCR-ABL and the gain-of-function and gain-of-resistance (T790M) mutants of epidermal growth factor receptor (EGFR) kinase.^{17,18} All these features support the development of Hsp90 inhibitors as targeted molecular therapeutics for cancer.^{19–21}

The past few years have witnessed a tremendous growth in the discovery of Hsp90-specific inhibitors belonging to several distinct chemical classes, which include benzoquinone ansamycins (e.g. geldanamycin derivatives), radicicol derivatives, purine-scaffold inhibitors, dihydroxyphenylpyrazoles, and small peptides.^{1,22,23} Among them, compound **1b** (17-AAG) and **4b** (17-dimethylaminoethylamino-17-demethoxygeldanamycin, 17-

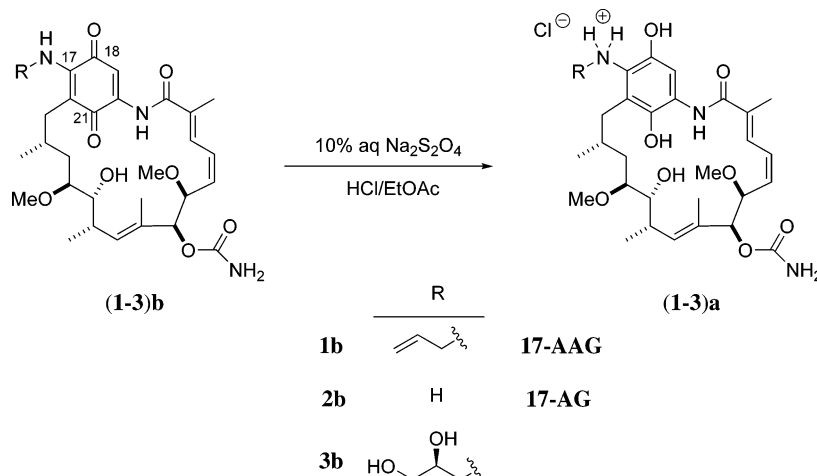
DMAG), derivatives of the natural product geldanamycin, are currently under evaluation in multiple clinical trials.^{24–27} 17-AAG inhibits Hsp90 by binding competitively to its N-terminal ATP binding site.^{28–30} This site is highly conserved among Hsp90 family proteins, whose human members include cytoplasmic Hsp90 α and Hsp90 β , ER-resident Grp94, and mitochondrial tumor necrosis factor receptor-associated protein 1 (Trap1). The Hsp90 chaperone complex facilitates the folding of client proteins through coupled cycles of ATP hydrolysis. Thus, inhibition of the ATPase activity results in misfolding and degradation of client proteins via the ubiquitin-proteasome pathway^{31–34} and in turn leads to growth arrest or apoptosis in cancer cells.^{2,4} Remarkably, 17-AAG displays selective cytotoxicity toward a broad range of cancer cells in vitro, inhibiting tumor cell growth at concentrations up to 1000-fold lower than those required for growth inhibition of normal cells.^{20,21,35} Furthermore, 17-AAG and its metabolites accumulate in tumor tissues at pharmacologically active concentrations in animal xenograft models.³⁵

Although 17-AAG is a potent inhibitor of Hsp90, it suffers from pharmacological deficiencies including poor solubility and complex organic formulations, with patient safety concerns. We initially hypothesized that hydroquinone analogues of 17-amino-17-demethoxygeldanamycin (17-AG) could be derivatized as phenol esters with improved solubility. The nonderivatized hydroquinone analogues were believed to be unstable, as Schnur and colleagues reported that hydroquinone derivatives of geldanamycin and its 17-azetidinyll analogue suffer from rapid oxidation.^{36,37} However, further studies revealed that the hydroquinone of 17-AAG can be isolated as the hydrochloride salt. Protonation of the aniline nitrogen in 17-AAG hydroquinone decreases electron density in the aromatic ring, thus reducing the oxidative potential of the hydroquinone. The salt can be purified and stored at low temperatures under N₂ atmosphere as a solid, demonstrates high aqueous solubility (≥ 250 mg/mL), and remains stable in acidic aqueous buffers (pH 3, > 10 h). The hydroquinone salt **1a** has since been named IPI-504. On the basis of the X-ray crystal structures of Hsp90 bound to

* Corresponding author. Telephone: 617-453-1000, Fax: 617-453-1001. E-mail: james.porter@ipi.com.

[†] These authors contributed equally to this work.

Scheme 1



geldanamycin or 17-DMAG, we proposed that **1a** could bind to and inhibit Hsp90.^{28–30}

Hydroquinone **1a** binds to human Hsp90 as well as canine Grp94 and shows activity against the human cancer cell lines SKBR3 and SKOV3. We also report the synthesis (Scheme 1) of additional hydroquinone derivatives of 17-AG and the evaluation of these compounds in both biochemical and cellular assays. The hydroquinone derivatives of two physiological metabolites of 17-AAG, **2a** and **3a**, exhibit similar affinity for Hsp90 compared to their quinone counterparts **2b** and **3b**.^{35,38} Reduction of quinone and subsequent preparation of the hydrochloride salt addresses the solubility limitations of 17-AAG and may represent a general approach to improve the physicochemical properties of quinone-based therapeutic agents.

Results

Chemistry. Various hydroquinone derivatives of 17-AG were isolated as hydrochloride salts. Specifically, **1b** (17-AAG) was reduced to the corresponding hydroquinone by sodium hydro-sulfite in a biphasic mixture of ethyl acetate and water (Scheme 1).^{36,37,39} The reaction progress can be followed by visual inspection of the vibrant purple color (quinone) transitioning to a yellow color (hydroquinone). The organic layer was separated and treated with a hydrochloride solution in ethyl acetate. The hydroquinone hydrochloride salt **1a** precipitated to give a pale yellow powder in high purity. The hydroquinone hydrochloride salt was found to be less prone to air oxidation and more soluble (250–275 mg/mL) than the free base (7–11 mg/mL). The yellow powder can be stored under inert atmosphere at –20 °C for >1 year without decomposition; however, storage at 22 °C leads to oxidation and formation of a pink powder over several days. In contrast, **1b** cannot be prepared as a hydrochloride salt and has limited aqueous solubility (0.02–0.05 mg/mL).

In vivo, **1b** is readily metabolized to diol **3b** and the dealkylated analogue **2b** (17-amino-17-demethoxygeldanamycin, 17-AG).^{35,38} The corresponding hydroquinone hydrochloride derivatives **3a** and **2a** were prepared from these two metabolites. Both compounds **2a** and **3a** exhibited similar solubility and stability profiles as hydroquinone **1a**. However, the aqueous solubility of the free base of **3a** resulted in extraction difficulties and low isolated yield after the biphasic reduction step.

In cellular assays, the hydroquinone species exist in redox equilibria with the quinone species.^{35,40} To prevent oxidation of hydroquinone derivatives in biochemical and cellular assays, we designed reduced analogues **5** and **6** that are locked in the hydroquinone oxidation state (Figure 1). Treatment of 17-AAG

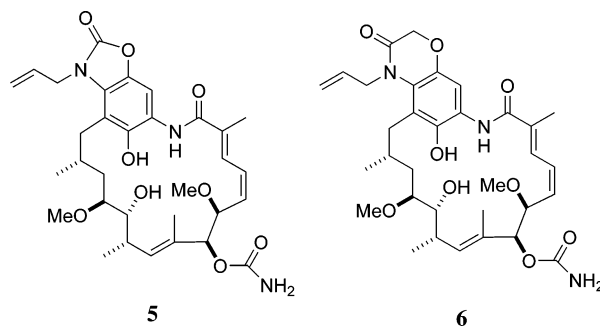
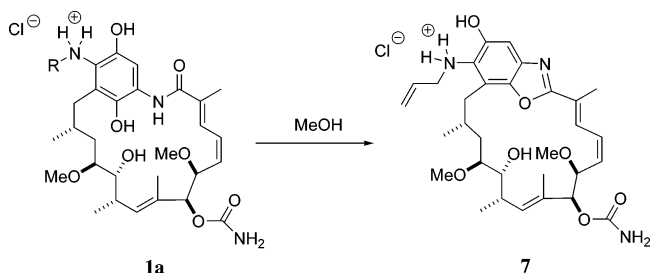


Figure 1. Chemical modification of the C-18 phenol leads to stabilized or “locked” hydroquinones **5** and **6**.

Scheme 2



hydroquinone with triphosgene provided hydroquinone carbamate **5** along with several other acylated products.⁴¹ The hydroquinone **1a** can also be acylated with bromoacetyl chloride at the 17-amino position and then treated with base to facilitate the alkylation and cyclization via the 18-phenol to yield hydroquinone amide **6**. The resulting locked compounds were stable during chromatography purification and exhibited no evidence of hydrolysis and oxidation during analysis. Monoalkylated ethers at the 18-phenol position of compound **1a** have also been prepared, but are rapidly oxidized upon purification.

A minor impurity observed in the synthesis of compound **1a** is benzoxazole analogue **7** (Scheme 2). Prolonged exposure of **1a** to acid resulted in increasing levels of intramolecular condensation and dissolution in methanol resulted in complete conversion to benzoxazole **7**. Similar to reduced analogues **5** and **6**, compound **7** is locked in the hydroquinone oxidation state and is stable.

Biological Data. The newly synthesized analogues **1a–7** were tested for their ability to bind to purified human Hsp90 (mixture of α and β isoforms) and canine Grp94 proteins using a fluorescence polarization (FP)-based competition binding

Table 1. Apparent Binding Affinity for Human Hsp90 and Canine Grp94

| Compound | R | EC ₅₀ ^a | |
|---------------------|---|-------------------------------|--------------------------|
| | | Hsp90 | Grp94 |
| 1a | | 63 ± 13 nM | 119 ± 18 nM ^b |
| 1b (17-AAG) | | 119 ± 23 nM | 124 ± 53 nM |
| 2a | H | 34 ± 13 nM | 48 ± 6 nM ^b |
| 2b (17-AG) | H | 34 ± 6 nM | 48 ± 14 nM |
| 3a | | 91 ± 24 nM | 131 ± 14 nM ^b |
| 3b | | 66 ± 17 nM | 72 ± 17 nM |
| 4b (17-DMAG) | | 62 ± 29 nM | 65 ± 9 nM |
| 5 | — | 603 ± 60 nM ^b | ND |
| 6 | — | 541 ± 97 nM ^b | ND |
| 7 | — | > 10 μM | > 10 μM |
| ADP | — | 87 ± 13 μM | 21 ± 4 μM ^b |
| ATP | — | 1.50 ± 0.16 mM | 19 ± 5 μM |

^a Unless otherwise noted, the values represent average ± standard deviation from several experiments ($n \geq 2$). ^b For these compounds ($n = 1$), EC₅₀ ± asymptotic standard errors from fitting the competition curves (triplicate data points) with four-parameter logistic function are reported. ND = Not determined.

assay.^{42,43} This assay utilized a boron difluoride dipyrromethene (BODIPY) labeled geldanamycin analogue (BODIPY-AG) as a probe and measured fluorescence polarization upon binding of the probe to a protein. Hsp70, another chaperone protein with a structurally distinct ATP binding site, was used as a negative control. No significant binding of BODIPY-AG to Hsp70 was observed at concentrations up to 10 μM (data not shown). The apparent binding affinities (EC₅₀) of various compounds for Hsp90 were determined in a competitive manner and are summarized in Table 1. To prevent oxidation of the hydroquinone compounds (**1–3a**) in neutral pH buffer, binding assays were performed in parallel with the quinone compounds (**1–3b**) in an inert N₂ environment (see Experimental Section).

The reduced hydroquinone **1a** exhibited a ~2-fold higher apparent affinity for human Hsp90 compared with quinone **1b** (EC₅₀ = 63 ± 13 nM and 119 ± 23 nM, respectively).³⁵ The majority (>60%) of compound **1a** remained reduced over the incubation period (3 h) at 30 °C, as confirmed by LC-MS. The observed EC₅₀ for **1b** is in good agreement with the reported value of 110 nM measured using recombinant human Hsp90α at 4 °C.⁴³ Similar binding affinities were determined using individual human Hsp90 α and β isoforms at 4 or 30 °C (data not shown).

Quinone **1b** was shown to dissociate from human Hsp90 with a first-order rate constant of 0.031 ± 0.003 min, i.e., a half-life ($t_{1/2}$) of 22 min at 37 °C (Figure 2). While the dissociation kinetics for hydroquinone **1a** was not determined, its increased affinity for Hsp90 relative to **1b** would suggest equal or slower rate of dissociation. Previous studies by Carreras et al. have reported a $t_{1/2}$ of ~2 min for dissociation of **1b** from the isolated human Hsp90α N-terminal domain (residues 9–236).⁴⁴ The difference may be explained by stabilization of the ligand binding conformation by multiple domain interactions within Hsp90. To search for further stabilization by co-chaperone proteins in a high affinity Hsp90 complex,²⁰ the dissociation kinetics of **1b** from presumed Hsp90 chaperone complex(es) in normal human dermal fibroblast (NHDF) and SKBR3 cell lysates were also determined. Identical $t_{1/2}$ values of 20 min were observed in both cases (data not shown). Thus we did not find evidence for a cancer cell (i.e., SKBR3)-specific Hsp90

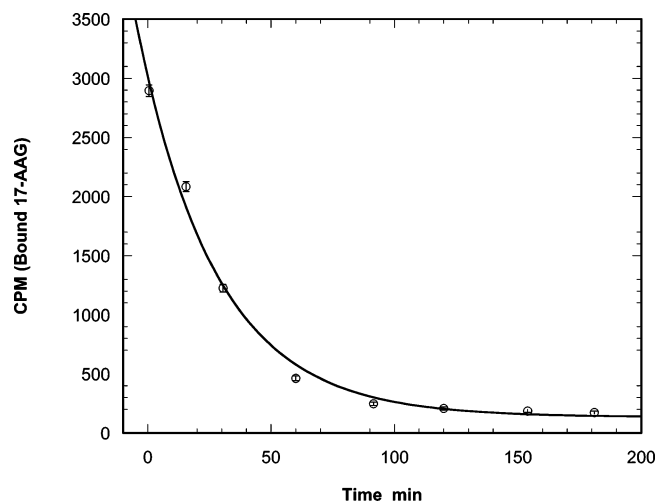


Figure 2. Dissociation of **1b** from human Hsp90 protein. Open circles (○) represent [³H]-17-AAG counts from the flow-through protein fractions as a function of incubation time in the dissociation reaction.

chaperone complex that exhibits different kinetic behavior than Hsp90 present in normal cell (i.e., NHDF) lysate.²⁰ One possible caveat, however, is that the Hsp90 chaperone complex might be disrupted under the experimental conditions.

Compounds **2b** and **3b** are two major metabolites of **1b** produced by liver enzymes under physiological conditions.^{35,38} These compounds and their hydroquinone derivatives **2a** and **3a** were shown to bind to Hsp90 protein (Table 1). Here the results should be interpreted with caution, as we assumed, given the stability of **1a**, that compounds **2a** and **3a** remained in the reduced state throughout the assay period, which had not been directly verified by LC-MS. Nonetheless, compounds **2a** and **2b** exhibited essentially the same affinity for Hsp90 (EC₅₀ = 34 ± 13 nM and 34 ± 6 nM, respectively), while the hydroquinone derivative of the diol metabolite **3a** exhibited similar, if slightly weaker, affinity relative to its quinone counterpart **3b** (EC₅₀ = 91 ± 24 nM and 66 ± 17 nM, respectively). The high affinity of compound **2b** (17-AG) is consistent with previous report of an IC₅₀ of 37 nM (compared with 31 nM

Table 2. Biological Activity of Hydroquinone and Quinone Compounds on SKBR3 and SKOV3 Cell Lines

| compound | Hsp90 binding, EC ₅₀ (nM) | cytotoxicity GI ₅₀ (nM) ^a | | Her2 degradation EC ₅₀ (nM) ^a | | Hsp70 induction EC ₅₀ (nM) ^a | |
|---------------------|--------------------------------------|---|------------|---|-------------|--|------------------|
| | | SKBR3 | SKOV3 | SKBR3 | SKOV3 | SKBR3 | SKOV3 |
| 1a | 63 ± 13 | 22 ± 4 | 52 ± 14 | 20 ± 2 | 27 ± 18 | 22 ± 4 | 16 ± 7 |
| 1b (17-AAG) | 119 ± 23 | 17 ± 3 | 15 ± 4 | 35 ± 10 | 19 ± 8 | 22 ± 5 | — |
| 2a | 34 ± 13 | 50 ± 8 | 17 ± 2 | 8 ± 2 | 31 ± 12 | 58 ± 58 | 10 ± 4 |
| 2b (17-AG) | 34 ± 6 | 25 ± 10 | 14 ± 1 | 8 ± 2 | 53 ± 6 | 17 ± 10 | 6 ± 2 |
| 3a | 91 ± 24 | 832 ± 220 | 1107 ± 327 | 321 ± 95 | 756 ± 608 | 102 ± 53 | >10 ⁴ |
| 3b | 66 ± 17 | 724 ± 128 | 2022 ± 777 | 141 ± 77 | 4585 ± 1003 | 140 ± 15 | 853 ± 297 |
| 4b (17-DMAG) | 62 ± 29 | 29 ± 8 | 32 ± 10 | 8 ± 4 | 46 ± 24 | 4 ± 2 | 14 ± 7 |
| 5 | 603 ± 60 | 583 ± 87 | 1241 ± 593 | 1046 ± 532 | 742 ± 338 | 384 ± 32 | 2283 ± 1788 |
| 6 | 541 ± 97 | 739 ± 231 | 726 ± 374 | 190 ± 109 | 415 ± 109 | 311 ± 81 | 1005 ± 579 |
| 7 | >10 ⁴ | 1779 ± 158 | 371 ± 251 | 585 ± 363 | 435 ± 179 | — | 3229 ± 2408 |

^a GI₅₀ denotes the concentration of compound at which 50% of cell growth is inhibited, whereas EC₅₀ represents the concentration where signal = (maximum – minimum)/2.

for **1b**) for Her2 protein depletion in SKBR3 cells^{36,37} and furthermore may explain the accumulation of **2b** in tumor tissues.³⁵

To corroborate that the measured affinities of the hydroquinone compounds (**1–3a**) are not the result of oxidation to their corresponding quinone derivatives under the experimental conditions, “locked” hydroquinone compounds **5** and **6** were tested and shown to bind to Hsp90, albeit with weaker affinity (EC₅₀ = 603 ± 60 nM and 541 ± 97 nM, respectively) compared with compound **1a**, suggesting that the hydroquinone derivatives are active per se. The weaker binding activities of compounds **5** and **6** can be interpreted on the basis of structure–activity relationships.

A minor impurity isolated during the synthesis of **1a**, benzoxazole **7**, was also tested for its ability to bind to Hsp90. Compound **7** results from an acid-catalyzed condensation between the C-21 phenol and the ansamycin amide (Scheme 2), providing a more rigid benzoxazole ring. Interestingly, benzoxazole **7** did not exhibit any affinity for Hsp90 up to 10 μM concentration.

Many of the known Hsp90 inhibitors also target Grp94, the ER homologue of Hsp90 that assists the folding of membrane and secreted proteins. A strong correlation was observed between the binding affinities of the analogues for Hsp90 and Grp94 (Table 1). Specifically, compound **1a** binds to Grp94 with an EC₅₀ of 119 ± 18 nM, slightly weaker than the EC₅₀ of 63 ± 13 nM it exhibits toward Hsp90.³⁵ These results suggest that inhibition of Grp94 may in part account for the cellular responses to geldanamycin derivatives. In agreement with previous literature reports, Hsp90 binds to ATP with a weaker affinity compared to ADP (EC₅₀ = 1.50 ± 0.16 mM and 87 ± 13 μM, respectively),^{45,46} whereas Grp94 binds to both nucleotides with identical affinity (21 ± 4 μM and 19 ± 5 μM, respectively).⁴⁷

To link the binding affinity of each compound to cellular activity, three in vitro assays were set up using the human cancer cell lines SKBR3 and SKOV3. The assays measured the effects of analogues on the degradation of Her2, up-regulation of Hsp70, and cytotoxicity. Her2, a member of the EGFR kinase family, is one of the most sensitive Hsp90 client proteins. In fact, 17-AAG causes the proteasomal degradation of this protein at nanomolar concentrations in SKBR3 cells.⁴⁸ Ansamycins also inhibit the association of Hsp90 with heat shock factor-1 (HSF-1), which induces the mRNA and protein levels of Hsp70. This increase in Hsp70 level has been used as a surrogate marker in 17-AAG clinical trials.⁴⁹ The levels of Her2 and Hsp70 proteins in both SKBR3 and SKOV3 cell lines were monitored using immunoassays after treatment with increasing concentrations of each compound for 24 h. The cytotoxic effects of the

compounds were evaluated after 72 h treatment using Alamar Blue, a marker of mitochondrial function.

The cellular activities (cytotoxicity GI₅₀ as well as EC₅₀ for Her2 protein degradation and Hsp70 induction) of most compounds, with the exception of **3a** and **3b**, are comparable to their apparent binding affinity for Hsp90 (Table 2). These results indicate that the major 17-AAG metabolites, 17-AG hydroquinone and quinone **2a** and **2b**, bear similar pharmacological effects compared to the parent compounds **1a** and **1b**. However, diol compounds **3a** and **3b** exhibit weaker cellular activities than would be expected from their binding affinity. This may reflect either low cellular uptake, slow accumulation, or susceptibility to further metabolism of these particular compounds in cells. It should be noted that no difference in cellular activity was detected between hydroquinone compounds (**1–3a**) and their respective quinone counterparts (**1–3b**). The hydroquinone compounds (**1–3a**) are likely oxidized rapidly in cell culture medium (pH 7.4). Furthermore, our recent findings demonstrate that a redox equilibrium between the hydroquinone **1a** and quinone **1b** is reached inside cells regardless of whether cells are treated with the reduced or oxidized compound.³⁵

In light of these findings, the cellular activities of the “locked” hydroquinone compounds **5** and **6** are especially interesting since their oxidation is prevented through chemical modification of the C-18 phenol group. The EC₅₀ values for Her2 degradation and Hsp70 induction are again comparable to their apparent binding affinities (Table 2), suggesting that the measured affinities for this series of 17-AG derivatives correlate with their cellular activities, as shown in Figure 3.

Discussion

The hydroquinone derivative **1a** binds to Hsp90 and Grp94 with high affinity.³⁵ The observed tight binding can be rationalized by examining the crystal structure of human Hsp90 in complex with **4b** (17-DMAG) at 1.75 Å resolution.²⁸ The quinone oxygen atom at C-18 position of the ligand is within hydrogen bonding distance of a structured water molecule, which itself is hydrogen bonded to the δ-O atom of residue N51 (numbered according to human Hsp90α). The other quinone oxygen at C-21 of **4b** is positioned 3.0 Å away from the ε-N atom of residue K112. The quinone moiety of **1b** would mimic these same interactions when bound to Hsp90. In comparison, the phenolic oxygens of the hydroquinone **1a** would differ in their hydrogen bonding capability by a more Lewis basic oxygen lone pair as well as a longer α C–O bond than the π C–O in the corresponding quinone. The crystal structure also reveals that the 17-N atom of **4b** is within hydrogen bonding distance (3.2 Å) to one of the carboxylate O atoms of residue

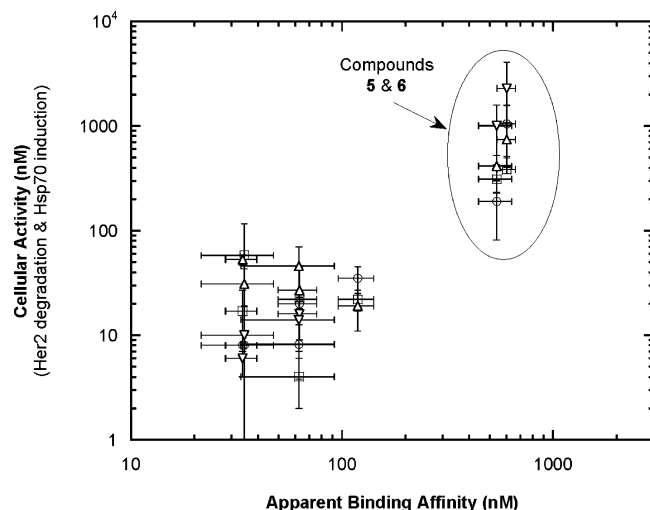


Figure 3. Correlation between apparent binding affinity and cellular activity (EC_{50}). Open circles (○) and squares (□) represent Her2 degradation and Hsp70 induction, respectively, in SKBR3 cells; open triangles (△) and inverted triangles (▽) represent Her2 degradation and Hsp70 induction in SKOV3 cells. Compounds **3a** and **3b** are omitted due to their poor cellular activities.

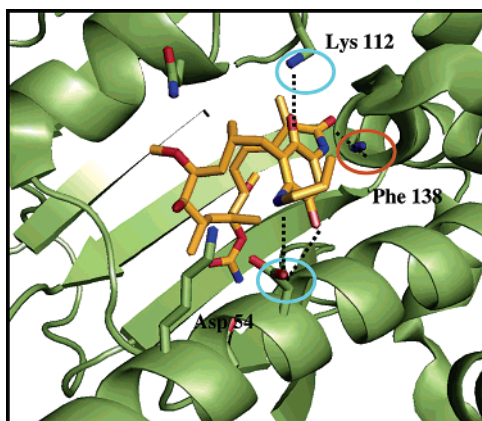


Figure 4. Molecular modeling of **1a** (gold) bound to Hsp90 (green). Hydrogen bonding interactions (blue circles) are available to **1a** through K112 and D54; and the ansamycin C-1 amide carbonyl could hydrogen bond to the backbone nitrogen of F138 on Hsp90 (orange circle). Ligand coordinates were built by analogy to the deposited X-ray crystal structure of 17-DMAG bound to Hsp90 (PDB code 1OSF), minimized using Chem3D (CambridgeSoft) and docked manually using pymol (DeLano Scientific).

D54. Although the vinylogous NH of the 17-(2-propenylamino) substituent group on **1b** would be a better H-bond donor than a typical aniline NH, an intramolecular H-bond between the 17-nitrogen lone pair and the C-18 phenol OH of **1a** should increase the H-bond donor characteristics of its 17-aniline NH. Such intramolecular H-bonding between the C-18 phenol OH and the 17-N is indeed suggested by preliminary NMR experiments. Furthermore, the C-18 and C-21 phenol OH would also reside within hydrogen bonding distance to the carboxylate oxygens of D54 and the side chain amine of K112, respectively (Figure 4). We hypothesize that these subtle differences in hydrogen bonding capability contribute to the ~2-fold higher apparent affinity of the hydroquinone **1a** for Hsp90 compared with **1b** (Table 1 and Sydor et al.³⁵). Further support for this hypothesis is found in a recent report from Guo et al. that describes the molecular modeling of the hydroquinone into Hsp90 crystal structures.⁴⁰ The authors emphasized stronger hydrogen bonding interactions between the hydroquinone and key residues in the ATP-binding site of Hsp90, e.g. D54, K58,

K112, and suggested the hydroquinone as a more potent inhibitor of Hsp90 compared with **1b**.

The physiological metabolite **2b** and its hydroquinone **2a** show comparable binding affinity for human Hsp90, whereas the diol metabolites **3a** and **3b** exhibit a slight difference in binding affinity favoring the quinone compound **3b**. Although these results may be interpreted as the result of oxidation of the hydroquinone compounds to quinones, thus giving similar apparent binding affinities, the fact that >60% of compound **1a** remains reduced under identical assay conditions (pH 7.3, ≥ 3 h at 30 °C in an anaerobic glovebox) leads us to assume otherwise. As discussed above, subtle differences in H-bonding characteristics between the quinone and hydroquinone compounds apply to these metabolites as well. The various substituent groups at the 17-position may contribute to the energetics of H-bonding, thus leading to the observed differences in binding affinities.

Locked hydroquinone analogues **5** and **6** have ~10-fold weaker apparent affinity for Hsp90 than compound **1a**. These results confirm that the quinone oxidation state is not a prerequisite for Hsp90 binding, as these compounds are restricted by chemical modification to the reduced form. Our findings are further corroborated by recent reports of structurally related compounds radanamycin and a phenolic ansamycin derivative (KOSN1559), which contain the 18-OH group and function as inhibitors of Hsp90.^{50,51} Interestingly, the ansamycin macbecin has been isolated in the hydroquinone form and demonstrates antitumor activity.⁵² The weak binding affinity of compounds **5** and **6** may be caused by the loss of H-bonding of the 17-NH, the 18-OH, or the 18-O lone pair. Nevertheless, these locked compounds are able to undergo the trans–cis isomerization and conformational changes to the C-shape ansamycin ring preferred for Hsp90 binding.^{28,30,53} It has been hypothesized that a *cis*-amide isostere or compound that is restricted to a C-shape conformation could bind favorably to Hsp90.^{53,54} The rigid conformation of benzoxazole **7** could potentially access this C-shape conformation but may lack key H-bonding interactions that **1a** possesses. However, the complete lack of affinity of **7** for Hsp90 may be indicative of its inability to access the C-shape conformation.

Using our FP competition binding assay, K_i values of 30 nM and 60 nM could be calculated for compound **1a** and **1b**, respectively, by assuming that 100% of human Hsp90 is active and interacts with 1 ligand per binding site (see Supporting Information). However, the binding affinity of **1b** for Hsp90 we report is 10- to 20-fold higher than several previously reported values determined using methods such as filter binding with [³H]-17-AAG ($K_d = 0.6 \mu\text{M}$),⁴⁴ fluorescence polarization ($IC_{50} = 1.27 \mu\text{M}$),⁵⁵ SPA competition with [³H]-17-AAG ($K_d = 0.6 \mu\text{M}$),⁵⁶ competition with immobilized geldanamycin ($EC_{50} = 1 \mu\text{M}$ and $0.6 \mu\text{M}$),^{20,57} and competition with biotin-GDM for binding to adsorbed Hsp90 ($IC_{50} = 0.8 \mu\text{M}$).³⁹ This apparent discrepancy may be explained by the presence of the nonionic detergent Nonidet P-40 (0.01%) in our assay conditions. Using a spin column assay, we have shown that the presence of NP-40 increases the binding affinity between Hsp90 and **1b** by ~20-fold (see Supporting Information). Moreover, NP-40 increases the fraction of Hsp90 capable of ligand binding by >2-fold, presumably by favoring an active protein conformation.

Our results also show a good correlation between Hsp90 binding affinity and cellular activities for a series of compounds (Figure 3). However, previous literature on geldanamycin classes of Hsp90 inhibitors reported either poor correlation between binding affinity and cytotoxicity (SKBR3)^{51,56} or a potency gap

between biochemical binding and Her2 degradation assays.³⁹ In addition, the presence of NP-40 has been reported to stabilize the ATP-dependent Hsp90-p23 association in both purified protein system and in co-immunoprecipitation experiments from reticulocyte lysate.^{58,59} Thus the assay conditions used in the current study may in fact represent a more physiologically relevant measure of Hsp90 binding activity.

It is worth noting that similar EC₅₀ values were obtained for the 17-AG analogues (**1a–2b**, **4b–6**) in Hsp90 binding and cellular assays (Table 2), even though these inhibitors must compete with high levels of endogenous ATP and ADP for binding. This is often the reason ATP-competitive inhibitors give higher EC₅₀ values in cellular assays than in biochemical binding assays. Possible explanations for our observations include, but not limited to, the preferential accumulation of **1b** within cells,²¹ or alternatively, higher affinity of **1b** for Hsp90 chaperone complex in cancer cells compared to purified Hsp90 protein.²⁰ While we have so far been unable to identify a high affinity Hsp90 chaperone complex in cancer cells, the exact mechanism(s) leading to tumor-specific accumulation of **1a/1b** and their metabolites remains to be elucidated.

Grp94 shares 44% sequence identity (62% similarity) with Hsp90 (α or β), particularly in the N-terminal ATP binding domain. However, Grp94 exhibits a pattern of binding affinities for adenosine nucleotides that is distinct from that of Hsp90, a result confirmed by our own findings.⁴⁷ On the basis of this and structural studies on Grp94, Nicchitta and colleagues hypothesized that, unlike Hsp90, the chaperone function of Grp94 depends on the presence or absence of a nucleotide ligand at the N-terminal site, but not on its phosphorylation state (i.e. ATP or ADP).^{60–62} In another report, however, the ATPase activity of Grp94 is found to be required for the maturation of at least a specific subset of client proteins, e.g., toll-like receptors (TLR), as a catalytic point mutant (E103A) of Grp94 is unable to restore TLR export to cell surface in a Grp94-deficient pre-B cell line.⁶³ The detailed mechanism of Grp94 chaperone function and the consequences of inhibition by geldanamycin derivatives thus requires further investigation.

Finally, we have recently demonstrated that hydroquinone **1a** and quinone **1b**, as well as compound **2a** and **2b**, exist in redox equilibria *in vivo*.³⁵ The relative affinities of these compounds suggest that, in previous clinical trials with 17-AAG, it is the combined effects of the hydroquinone and quinone forms of 17-AAG and the metabolites that collectively exert antitumor activity, possibly through multiple pathways involving Hsp90 family members.

Conclusions

The hydroquinone hydrochloride salt **1a** is a highly soluble and potent inhibitor of Hsp90 and Grp94. In addition, both the hydroquinone and quinone forms of 17-AAG and the metabolites show comparable binding affinities for Hsp90, lifting previous concerns that extensive metabolism of 17-AAG might offset its antitumor activity. In SKBR3 and SKOV3 cancer cell lines, these analogues elicit specific responses consistent with Hsp90 inhibition. While the detailed mechanism of action of these compounds remains the subject of ongoing investigations, their desirable pharmacological properties justify clinical development. To this end, the lead compound IPI-504 is under evaluation in Phase I clinical trials in multiple myeloma and gastrointestinal stromal tumors.⁶⁴

Experimental Section

Chemistry. Commercial reagents and solvents were used as received without further purification or drying. Technical grade

(~85%) sodium hydrosulfite (Na₂S₂O₄) was purchased from Sigma-Aldrich. A freshly prepared 10% aqueous solution (w/v) of Na₂S₂O₄ was used for quinone reduction. Geldanamycin was purchased from AG Scientific, and 17-AAG, 17-DMAG, and BODIPY-AG were synthesized as previously reported.^{43,65,66} Flash chromatography was run using silica gel (200–400 mesh) from Sorbent Technologies. Analytical liquid chromatography (HPLC) was performed on an Agilent 1100 HPLC system equipped with a Waters C18–Symmetry reverse-phase column (4.6 × 150 mm, 5 μ m). The mobile phases were acetonitrile (0.1% trifluoroacetic acid) and water (0.1% trifluoroacetic acid). The compounds were eluted with a gradient of 10% to 70% acetonitrile over 20 min, followed by 70% acetonitrile for 5 min, at a flow rate of 1 mL/min and detection wavelength at 254 nm. Infrared (IR) spectra were recorded on a Thermo-Nicolet 370 FT-IR spectrophotometer, ν_{\max} is reported in cm⁻¹. ¹H NMR spectra were recorded on a Bruker 400 spectrometer (400 MHz). Chemical shifts are reported in ppm with the solvent resonance as the internal standard (CHCl₃: δ 7.26). Data are reported as follows: chemical shift, integration, multiplicity (s = singlet, d = doublet, t = triplet, q = quartet, br = broad, m = multiplet), and coupling constants (Hz). ¹³C NMR spectra were recorded on a Bruker 400 spectrometer (100 MHz) with complete proton decoupling. Chemical shifts are reported in ppm with the solvent as the internal reference (CDCl₃: δ 77.0). High-resolution mass spectra (HRMS) were run at the Harvard University mass spectrometry facility using a Micromass LCT time-of-flight electrospray positive (ES⁺) spectrometer.

17-Allylamino-17-demethoxygeldanamycin Hydroquinone Hydrochloride 1a. To a solution of 17-allylamino-geldanamycin (17-AAG, **1b**) (13 g, 22 mmol, 1.0 equiv) in ethyl acetate (250 mL) at 22 °C was added 10% aqueous Na₂S₂O₄ (250 mL). The biphasic mixture was stirred vigorously until the purple solution turned yellow (1 h). The organic layer was separated, washed with 250 mL brine, and dried over magnesium sulfate. The organic solution was filtered then stirred at 22 °C under nitrogen atmosphere. The solution was acidified with hydrogen chloride in ethyl acetate (10 mL, 1.4 M) to pH 2–3 as a white suspension formed. The slurry was stirred for 10 min, filtered, and dried *in vacuo* to isolate the 17-AAG hydroquinone hydrochloride (**1a**) as an off-white solid (11 g, 18 mmol, 80% yield). HPLC purity: 99.6%; IR (neat): 3175, 2972, 1728, 1651, 1581, 1546, 1456, 1392, 1316, 1224, 1099, 1036 cm⁻¹; ¹H NMR (CDCl₃:d₆-DMSO, 6:1, 400 MHz): δ 10.20 (1H, br), 9.62 (2H, br), 8.53 (1H, s), 8.47 (1H, s), 7.74 (1H, s), 6.72 (1H, d, J = 11.6 Hz), 6.28 (1H, dd, J = 11.6, 11.2 Hz), 5.73 (1H, dddd, J = 17.2, 10.0, 3.2, 2.4 Hz), 5.53 (1H, d, J = 10.4 Hz), 5.49 (1H, dd, J = 10.8, 10.0 Hz), 5.32 (2H, s), 5.04 (1H, d, J = 4.8 Hz), 5.02 (1H, d, J = 16.0 Hz), 4.81 (1H, s), 4.07 (1H, d, J = 9.6 Hz), 3.67 (2H, d, J = 6.4 Hz), 3.31 (1H, d, J = 8.8 Hz), 3.07 (3H, s), 3.07–3.04 (1H, m), 2.99 (3H, s), 2.64 (1H, m), 2.52–2.49 (1H, m), 1.76 (3H, s), 1.61–1.39 (3H, m), 0.78 (3H, d, J = 6.4 Hz), 0.64 (3H, d, J = 7.2 Hz); ¹³C NMR (CDCl₃:d₆-DMSO, 6:1, 100 MHz): δ 167.3, 155.8, 143.3, 136.3, 135.0, 134.2, 132.9, 132.1, 128.8, 127.6, 125.9, 125.3, 123.7, 123.0, 115.1, 104.5, 80.9, 80.7, 80.1, 72.5, 56.2, 56.2, 52.4, 34.6, 33.2, 31.1, 27.2, 21.6, 12.1, 12.1, 11.7; HRMS calculated for C₃₁H₄₅N₃O₈ (M⁺ + H): 588.3285, Found 588.3273.

17-Amino-17-demethoxygeldanamycin Hydroquinone Hydrochloride 2a. To a solution of 17-aminogeldanamycin (17-AG, **2b**) (550 mg, 1.0 mmol, 1.0 equiv) in ethyl acetate (10 mL) at 22 °C was added 10% aqueous Na₂S₂O₄ (10 mL). The biphasic mixture was stirred vigorously until the purple solution turned yellow (50 min). The organic layer was separated, washed with 10 mL brine, and dried over magnesium sulfate. The organic solution was filtered then stirred at 22 °C under nitrogen atmosphere. The solution was acidified with hydrogen chloride in ethyl acetate (1 mL, 1.5 M) to pH 2–3 as a white suspension formed. The slurry was stirred for 10 min, filtered, and dried *in vacuo* to isolate the 17-AG hydroquinone hydrochloride **2a** as a bright yellow solid (520 mg, 0.90 mmol, 90% yield). HPLC purity: 98.6%; IR (neat): 3231, 2917, 2833, 1707, 1651, 1588, 1525, 1435, 1386, 1330, 1099, 1050 cm⁻¹; ¹H NMR (CDCl₃:d₆-DMSO, 6:1, 400 MHz): δ 9.30 (2H, br), 8.98

(1H, s), 8.58 (1H, br), 8.48 (1H, s), 7.74 & 6.95 (1H, s, rotamer), 6.75 (1H, d, $J = 10.8$ Hz), 6.33 (1H, t, $J = 11.2$ Hz), 6.15 & 5.64 (1H, br, rotamer), 5.66–5.51 (2H, m), 5.29 (2H, s), 4.91 & 4.85 (1H, s, rotamer), 4.10 (1H, dd, $J = 9.2, 8.8$ Hz), 3.37 (1H, dd, $J = 20.8, 8.8$ Hz), 3.18–3.11 (1H, m), 3.12 (3H, s), 3.03 (3H, s), 2.76–2.51 (3H, m), 1.81–1.73 (1H, m), 1.78 (3H, s), 1.59–1.50 (1H, m), 1.55 (3H, s), 0.79 (3H, d, $J = 6.4$ Hz), 0.69 (3H, d, $J = 7.2$ Hz); ^{13}C NMR (CDCl_3 : d_6 -DMSO, 6:1, 100 MHz) (Extra peaks due to rotamers): δ 167.5, 167.3, 155.8, 155.7, 146.3, 142.9, 136.4, 135.0, 133.9, 132.8, 132.0, 127.7, 125.8, 125.1, 123.2, 111.7, 108.6, 107.3, 104.2, 80.7, 80.5, 80.0, 72.4, 71.5, 56.1, 56.0, 34.4, 33.4, 33.3, 31.3, 21.8, 12.1, 12.0, 11.7; HRMS calculated for $\text{C}_{28}\text{H}_{41}\text{N}_3\text{O}_8$ ($\text{M}^+ + \text{H}$): 548.2972, Found 548.2971.

17-Amino-17-demethoxygeldanamycin 2b. The procedure for the synthesis of **2b** was adapted from literature reports.⁶⁷ To a solution of geldanamycin (5.6 g, 10 mmol, 1.0 equiv) in CH_2Cl_2 (150 mL) at 22 °C was added NH_3 in methanol (21 mL of a 7 M solution, 150 mmol, 15 equiv). The yellow solution turned purple and was stirred for 2.5 days. The reaction showed incomplete consumption of starting material by LCMS, so additional NH_3 in methanol (7 mL of a 7 M solution, 50 mmol, 5 equiv) was added. The reaction was stirred for an additional 3 days, and LCMS monitoring indicated complete consumption of geldanamycin. The reaction was diluted with CH_2Cl_2 (350 mL), quenched with water (150 mL), and acidified to pH 3.0 with 2 N HCl. The organic layer was separated, washed with water (100 mL), dried with magnesium sulfate, and concentrated. The residue was slurried at 55–60 °C for 30 min in acetone (80 mL) and then diluted with *n*-heptane (400 mL). The mixture was cooled to 5 °C with stirring, and a purple solid was isolated by filtration. The crude material was recrystallized by dissolving in 100 mL of acetone at 55–60 °C and then diluting with 200 mL of *n*-heptane. The mixture was cooled to 22 °C with stirring over 12 h and then at 5 °C for 2 h. The purple solid was isolated by filtration and rinsed with 50 mL *n*-heptane to give 17-aminogeldanamycin **2b** (5.2 g, 5.2 mmol, 95% yield). HPLC purity: 99.4%; IR (neat): 3497, 3469, 3420, 3329, 3196, 3133, 2931, 2889, 2826, 2350, 1728, 1686, 1616, 1553, 1463, 1442, 1364, 1316 cm^{-1} ; ^1H NMR (CDCl_3 , 400 MHz): δ 9.08 (1H, s), 7.21 (1H, s), 6.92 (1H, d, $J = 11.6$ Hz), 6.55 (1H, dd, $J = 11.6, 11.2$ Hz), 5.88 (1H, d, $J = 9.2$ Hz), 5.83 (1H, dd, $J = 10.8, 10.4$ Hz), 5.56 (2H, s), 5.12 (1H, s), 4.87 (2H, br), 4.32 (1H, br), 4.28 (1H, d, $J = 10.0$ Hz), 3.67 (1H, d, $J = 9.2$ Hz), 3.42 (1H, dd, $J = 8.8, 3.2$ Hz), 3.35 (3H, s), 3.25 (3H, s), 2.79–2.71 (2H, m), 2.01 (3H, s), 2.01–1.97 (1H, m), 1.89–1.67 (3H, m), 1.80 (3H, s), 1.00 (3H, d, $J = 6.8$ Hz), 0.97 (3H, d, $J = 6.2$ Hz); ^{13}C NMR (CDCl_3 , 100 MHz): δ 183.1, 180.3, 167.8, 156.1, 146.0, 140.4, 135.8, 135.0, 134.0, 133.0, 126.8, 126.6, 110.3, 108.5, 81.9, 81.2, 81.1, 72.2, 57.1, 56.8, 35.0, 34.7, 32.2, 28.7, 23.8, 12.8, 12.5, 12.2; HRMS calculated for $\text{C}_{28}\text{H}_{39}\text{N}_3\text{O}_8$ ($\text{M}^+ + \text{NH}_4$): 563.3081, Found 563.3081.

17-((S)-Amino-3,2-propanediol)-17-demethoxygeldanamycin Hydroquinone 3a. To a solution of 17-((S)-amino-3,2-propanediol)-17-demethoxygeldanamycin (**3b**) (680 mg, 1.1 mmol, 1.0 equiv) in ethyl acetate (20 mL) at 22 °C was added 10% aqueous $\text{Na}_2\text{S}_2\text{O}_4$ (10 mL). The biphasic mixture was stirred vigorously for 30 min and a yellow solid precipitated. The yellow solid was filtered and washed with ethyl acetate (2×20 mL). To the solid, 20 mL water was added until a cloudy yellow solution resulted, and then 30 mL ethyl acetate was added to precipitate a yellow solid (free base of hydroquinone, 325 mg). The yellow powder was dissolved in ethyl acetate (20 mL) with sonication and was acidified with hydrogen chloride in ethyl acetate (1 mL, 2.3 M) to pH 2–3 as a yellow suspension formed. The slurry was stirred for 10 min, filtered, and dried in vacuo to isolate the 17-AG propanediol hydroquinone hydrochloride **3a** as a bright yellow solid (120 mg, 0.18 mmol, 17% yield). HPLC purity: 90.8%; IR (neat): 3406, 3210, 2979, 2917, 1686, 1630, 1490, 1456, 1379, 1309, 1218, 1071, 1043 cm^{-1} ; ^1H NMR (CDCl_3 : d_6 -DMSO, 6:1, 400 MHz): δ 9.74 (1H, br), 8.70 (1H, s), 8.46 (1H, s), 7.71 (1H, s), 6.69 (1H, d, $J = 11.2$ Hz), 6.24 (1H, t, $J = 11.2$ Hz), 5.49–5.44 (2H, m), 5.37 (2H, s), 4.76 (1H, s), 4.26 (1H, br), 4.03 (1H, d, $J = 9.6$ Hz), 3.87 (1H, br), 3.50–3.39 (4H, m), 3.31 (1H, d, $J = 8.4$ Hz), 3.11–2.99 (1H,

m), 3.03 (3H, s), 2.94 (3H, s), 2.63 (1H, d, $J = 12.8$ Hz), 2.45–2.43 (2H, m), 1.73–1.70 (4H, m), 1.56–1.46 (2H, m), 1.47 (3H, s), 0.73 (3H, d, $J = 6.4$ Hz), 0.61 (3H, d, $J = 6.8$ Hz); ^{13}C NMR (CDCl_3 : d_6 -DMSO, 6:1, 100 MHz): δ 167.3, 155.8, 143.0, 136.5, 135.0, 134.0, 132.9, 132.1, 129.0, 125.8, 122.4, 115.8, 104.6, 80.8, 80.6, 80.0, 72.5, 66.2, 64.1, 56.2, 54.9, 34.5, 33.5, 33.4, 31.4, 27.2, 22.0, 20.4, 12.0, 11.9, 11.8; HRMS calculated for $\text{C}_{31}\text{H}_{47}\text{N}_3\text{O}_{10}$ ($\text{M}^+ + \text{H}$): 622.3339, Found 622.3339.

17-((S)-Amino-3,2-propanediol)-17-demethoxygeldanamycin 3b. To a solution of geldanamycin (5.0 g, 8.9 mmol, 1.0 equiv) in tetrahydrofuran (10 mL) at 22 °C was added (*S*)-3-amino-1,2-propanediol (3.5 mL, 45 mmol, 5.0 equiv). The yellow solution turned purple and was stirred for 2 h. The reaction was quenched with 0.1 N HCl (10 mL) and extracted with ethyl acetate (3 × 20 mL). The combined organic extracts were washed with water (30 mL), dried with magnesium sulfate, and concentrated. The crude material was purified by silica gel chromatography with a gradient of 1:1 hexanes:ethyl acetate, followed by 100% ethyl acetate, and then 10:1 ethyl acetate:methanol to isolate 17-amino-propane diol **3b** as a purple solid (4.0 g, 6.5 mmol, 73% yield). HPLC purity: 100%; IR (neat): 3490, 3434, 3308, 3210, 2972, 2937, 2882, 2364, 1728, 1686, 1637, 1567, 1490, 1358, 1246, 1106, 1043 cm^{-1} ; ^1H NMR (CDCl_3 : d_6 -DMSO, 6:1, 400 MHz): δ 9.00 & 8.80 (1H, s, rotamer), 6.73–6.70 (2H, m), 6.35–6.30 (2H, m), 5.65 (1H, d, $J = 9.6$ Hz), 5.55 (1H, t, $J = 10.4$ Hz), 5.28 (2H, br), 5.13 (1H, s), 4.92 & 4.88 (1H, s, rotamer), 4.65 (1H, br), 4.06 (1H, d, $J = 10.0$ Hz), 3.98 (1H, d, $J = 6.8$ Hz), 3.87–3.76 (2H, m), 3.58–3.55 (1H, m), 3.39 (1H, d, $J = 5.2$ Hz), 3.20 (1H, d, $J = 9.2$ Hz), 3.19–2.82 (8H, m), 2.48 (1H, t, $J = 7.2$ Hz), 2.19 (1H, d, $J = 13.6$ Hz), 1.81–1.71 (4H, m), 1.55 (3H, s), 1.39–1.36 (1H, m), 1.16–1.14 (1H, m), 0.76–0.64 (6H, m); ^{13}C NMR (CDCl_3 : d_6 -DMSO, 6:1, 100 MHz): δ 176.9, 167.8, 157.5, 155.9, 134.7, 133.9, 132.7, 132.2, 126.1, 125.3, 110.2, 103.6, 97.0, 80.9, 80.8, 80.6, 73.1, 71.5, 68.3, 56.3, 56.0, 47.1, 34.5, 32.3, 31.6, 27.7, 22.7, 12.3, 12.0, 11.7; HRMS calculated for $\text{C}_{31}\text{H}_{45}\text{N}_3\text{O}_{10}$ ($\text{M}^+ + \text{H}$): 620.3183, Found 620.3173.

17-Allylamino-17-demethoxygeldanamycin Hydroquinone Carbamate 5. To a solution of 17-AAG (**1b**) (910 mg, 1.6 mmol, 1.0 equiv) in ethyl acetate (18 mL) at 22 °C was added 10% aqueous $\text{Na}_2\text{S}_2\text{O}_4$ (18 mL). The biphasic mixture was stirred vigorously until the purple solution turned yellow (1 h). The organic layer was separated and dried over magnesium sulfate. The organic solution was filtered and then stirred at 22 °C under nitrogen atmosphere. A solution of triphosgene (460 mg, 1.6 mmol, 1.0 equiv) in ethyl acetate (2 mL) was added, and a white suspension formed. The slurry was stirred for 2 h and filtered to remove the hydroquinone salt. The filtrate was then concentrated and purified by silica gel chromatography using a gradient of 4:1 hexanes:ethyl acetate, 1:1 hexanes:ethyl acetate, 1:2 hexanes:ethyl acetate, followed by 100% ethyl acetate. Mixed fractions of desired product and another impurity were combined and concentrated to a crude yellow oil (130 mg). This material was dissolved in methanol and purified by preparatory LC (Waters Delta 600 HPLC equipped with a Waters C18–Symmetry (19 × 50 mm, 5 μm) reverse-phase column). The mobile phases were acetonitrile and water (0.1% formic acid). The compounds were eluted with 10% acetonitrile for 2 min, a gradient of 10% to 100% acetonitrile over 5 min, and 100% acetonitrile for 2 min, at a flow rate of 1 mL/min and detection wavelength at 254 nm. Concentration of purified fractions yielded carbamate **5** as a pale yellow powder (45 mg, 0.073 mmol, 5% yield). HPLC purity: 99.3%; IR (neat): 3420, 3343, 2972, 2924, 2812, 2357, 2329, 1742, 1686, 1644, 1637, 1525, 1477, 1427, 1372, 1315, 1106, 1057, 1015, 931 cm^{-1} ; ^1H NMR (CDCl_3 , 400 MHz): δ 8.45 (1H, s), 8.28 (2H, s), 6.88 (1H, d, $J = 11.6$ Hz), 6.36 (1H, dd, $J = 11.2, 10.8$ Hz), 5.97–5.88 (1H, m), 5.85 (1H, d, $J = 10.0$ Hz), 5.67 (1H, dd, $J = 10.8, 10.0$ Hz), 5.29 (1H, d, $J = 10.4$ Hz), 5.14 (1H, d, $J = 17.2$ Hz), 5.01 (1H, s), 4.86 (1H, ddd, $J = 17.6, 4.4, 2.0$ Hz), 4.46 (1H, dd, $J = 17.6, 4.4$ Hz), 4.32 (1H, d, $J = 10.0$ Hz), 3.65 (1H, dd, $J = 9.2, 8.4$ Hz), 3.54–3.45 (2H, m), 3.36 (3H, s), 3.24 (3H, s), 2.85–2.81 (1H, m), 2.73 2.63 (2H, m), 1.88–1.84 (2H, m), 1.80 (3H, d, $J = 0.8$ Hz), 1.73–1.70 (1H, m), 1.70 (3H, s), 1.02–0.93 (3H, m), 0.90–0.86 (3H, m); ^{13}C NMR (CDCl_3 , 100

MHz): δ 167.2, 156.6, 155.8, 140.6, 137.0, 135.8, 133.6, 132.6, 132.6, 132.0, 127.3, 123.9, 123.8, 122.8, 117.5, 111.2, 100.4, 82.7, 80.9, 80.4, 74.8, 57.1, 56.9, 45.1, 35.1, 34.2, 32.4, 29.1, 22.8, 12.6, 12.5, 12.1; HRMS calculated for $C_{32}H_{43}N_3O_9$ ($M^+ + NH_4$): 631.3343, Found 631.3320.

17-Allylamino-17-demethoxygeldanamycin Hydroquinone Amide 6. To a solution of **1a** (2.0 g, 3.2 mmol, 1.0 equiv) in a 1:1 mixture of tetrahydrofuran:water (20 mL) was added bromoacetyl chloride (0.27 mL, 3.2 mmol, 1.0 equiv). The solution was stirred for 2 min, and then sodium carbonate (2.0 g, 19 mmol, 6.0 equiv) was added as a solid. The mixture was stirred for 1 h and then quenched with saturated sodium bicarbonate (15 mL), extracted with ethyl acetate (3×15 mL), and washed with brine (25 mL). The organic solution was dried with magnesium sulfate and concentrated to a residue. The crude material was purified by silica gel chromatography using a gradient of 1:1 hexanes:ethyl acetate, 1:2 hexanes:ethyl acetate, and then 1:4 hexanes:ethyl acetate to yield vibrant UV spot on TLC mixed with some 17-AAG. Another silica column was run with the same gradient to isolate pure hydroquinone amide **6** as a dark yellow solid (101 mg, 0.16 mmol, 5% yield). HPLC purity: 94.8%; IR (neat): 3413, 3350, 2917, 2840, 1665, 1602, 1532, 1469, 1379, 1316, 1218, 1183, 1113, 1043, 910, 903 cm^{-1} ; 1H NMR ($CDCl_3$, 400 MHz): δ 8.44 (1H, s), 8.34 (1H, s), 8.02 (1H, s), 6.87 (1H, d, $J = 11.2$ Hz), 6.30 (1H, dd, $J = 11.6$, 11.2 Hz), 5.88–5.79 (2H, m), 5.65 (1H, dd, $J = 10.8$, 10.4 Hz), 5.24 (1H, dd, $J = 13.2$, 0.6 Hz), 5.20 (1H, dd, $J = 6.0$, 0.8 Hz), 4.98 (1H, s), 4.72 (1H, dd, $J = 16.0$, 4.8 Hz), 4.57 (1H, d, $J = 14.0$ Hz), 4.32–4.27 (2H, m), 4.17 (1H, d, $J = 14.0$ Hz), 3.56 (1H, br), 3.43–3.41 (1H, m), 3.34 (3H, s), 3.22 (3H, s), 2.82–2.76 (1H, m), 2.70–2.65 (2H, m), 1.80–1.63 (3H, m), 1.78 (3H, s), 1.67 (3H, s), 0.94 (3H, d, $J = 7.2$ Hz), 0.80 (3H, d, $J = 6.0$ Hz); ^{13}C NMR ($CDCl_3$, 100 MHz): δ 168.5, 167.5, 156.6, 143.4, 139.9, 137.1, 133.7, 132.9, 132.4, 132.3, 127.4, 125.0, 124.8, 124.4, 119.4, 117.3, 105.4, 82.6, 80.9, 80.5, 74.8, 69.9, 57.0, 56.9, 50.8, 36.9, 35.0, 32.4, 29.6, 22.4, 12.6, 12.6, 12.2; HRMS calculated for $C_{33}H_{45}N_3O_9$ ($M^+ + NH_4$): 645.3500, Found 645.3530.

Benzoxazole 7. Hydroquinone hydrochloride **1a** (400 mg, 0.64 mmol, 1.0 equiv) was dissolved in methanol (3 mL) at 22 °C and stirred under nitrogen atmosphere for 72 h. Ethyl acetate was added (5 mL) until the solution turned turbid and then allowed to precipitate over 1 h. The precipitate was collected and washed with ethyl acetate (3×5 mL). The material was dried in vacuo to yield benzoxazole **7** as a yellow powder (270 mg, 0.45 mmol, 70% yield). HPLC purity: 98.1%; IR (neat): 3343, 3182, 2937, 2819, 1700, 1595, 1512, 1456, 1392, 1322, 1064, 854, 784, 540 cm^{-1} ; 1H NMR ($CDCl_3:d_6$ -DMSO, 6:1, 400 MHz): δ 10.28 (2H, br), 8.31 (1H, s), 7.31 (1H, br), 6.36 (1H, t, $J = 11.2$ Hz), 5.73 (1H, dddd, $J = 10.4$, 10.0, 9.6, 7.2 Hz), 5.53 (1H, t, $J = 10.8$ Hz), 5.39 (2H, s), 5.10 (1H, d, $J = 9.2$ Hz), 5.01 (1H, d, $J = 3.2$ Hz), 4.98 (1H, d, $J = 1.2$ Hz), 4.85 (1H, s), 4.05 (1H, d, $J = 8.8$ Hz), 3.64 (2H, d, $J = 7.2$ Hz), 3.36 (1H, dd, $J = 9.6$, 2.0 Hz), 3.04 (1H, d, $J = 8.4$ Hz), 2.97 (3H, s), 2.94 (3H, s), 2.58 (1H, dd, $J = 15.6$, 10.8 Hz), 2.28 (1H, dq, $J = 2.0$, 1.6 Hz), 1.95 (3H, s), 1.50 (3H, s), 1.40–1.23 (3H, m), 0.82 (3H, d, $J = 6.4$ Hz), 0.56 (3H, d, $J = 6.4$ Hz); ^{13}C NMR ($CDCl_3:d_6$ -DMSO, 6:1, 100 MHz): δ 165.1, 155.7, 147.9, 142.0, 141.7, 127.4, 124.3, 123.1, 119.9, 118.9, 103.8, 103.7, 83.5, 79.3, 77.7, 73.4, 59.5, 56.2, 55.3, 52.5, 35.0, 34.8, 32.8, 32.7, 31.5, 20.3, 20.1, 20.0, 13.5, 12.0, 11.9; HRMS calculated for $C_{31}H_{43}N_3O_7$ ($M^+ + H$): 570.3179, Found 570.3175.

Solubility Assay. Compounds (20–40 mg) were placed in 2.0 mL polypropylene microcentrifuge tubes and incubated with 100 μ L of a pH 3.3 citrate-buffered solution on an Eppendorf Thermomixer (1000 rpm, 25 °C). Due to the instability of **1a** and its free base, incubation times for these compounds were kept to a minimum to avoid excessive conversion to the quinone state. Samples of **1b** were incubated overnight. After incubation, samples were centrifuged at 20 800g for 2 min and syringe filtered through a 0.22 μ m PVDF membrane filter. Aliquots of the filtrates were diluted into DMSO/acetonitrile/trifluoroacetic acid (80:20:0.1) and kept at 4 °C until injected. Analysis was performed on an Agilent 1100 HPLC system equipped with a Waters Symmetry IS C18 column, (3.5 μ m,

2.1 \times 20 mm) with detection wavelength at 254 nm. The mobile phases consisted of water (0.1% trifluoroacetic acid) and acetonitrile (0.1% trifluoroacetic acid). The column was eluted with 10% acetonitrile (0.1% trifluoroacetic acid) for 0.5 min, followed by a gradient of 10% to 55% acetonitrile (0.1% trifluoroacetic acid) over 9.5 min, and 70% acetonitrile (0.1% trifluoroacetic acid) for 1 min at a flow rate of 1 mL/min. Peaks were identified and quantified relative to known standards; and the amounts of soluble compound were calculated.

Competition Binding Assay. Native human Hsp90 protein ($\alpha + \beta$ isoforms) isolated from HeLa cells (SPP-770) and recombinant canine Grp94 (SPP-766) were purchased from Stressgen Biotechnologies (Victoria, BC). The procedures of the FP-based binding assay were adapted from those described by Chiosis and colleagues.^{42,43} BODIPY-AG solution was freshly prepared in FP assay buffer (20 mM HEPES–KOH, pH 7.3, 1.0 mM EDTA, 100 mM KCl, 5.0 mM $MgCl_2$, 0.01% NP-40, 0.1 mg/mL *fresh* bovine γ -globulin (BGG), 1.0 mM *fresh* DTT, and Complete protease inhibitor (Roche Diagnostics, Indianapolis, IN)) from stock solution in DMSO. Binding curves were obtained by mixing equal volume (10 μ L) of the BODIPY-AG solution and serially diluted human Hsp90 (or Grp94) solution in a 384-well microplate (Corning #3676) to yield 10 nM BODIPY-AG, varying concentration of Hsp90 (0.10 nM–6.25 μ M monomer), and 0.05% DMSO. After 3 h incubation at 30 °C, fluorescence anisotropy ($\lambda_{Ex} = 485$ nm, $\lambda_{Em} = 535$ nm) was measured on an EnVision 2100 multilabel plate reader (Perkin-Elmer, Boston, MA). Competition curves were obtained by mixing 10 μ L each of a solution containing BODIPY-AG and Hsp90 (or Grp94), and a serial dilution of each compound freshly prepared in FP assay buffer from stock solution in DMSO. Final concentrations were 10 nM BODIPY-AG, 40 or 60 nM Hsp90 (or Grp94), varying concentration of each compound (0.10 nM–10 μ M), and $\leq 0.25\%$ DMSO. Because compounds (**1–3a**) oxidize easily at neutral pH, assays of these compounds were performed in parallel with the quinone compounds (**1–3b**) under nitrogen atmosphere in a LabMaster glovebox (M. Braun, Stratham, NH). Typically, Hsp90 protein solution and compound stock solutions were brought into the glovebox as frozen liquid, and binding mixtures were prepared in FP assay buffer deoxygenated by repeated cycles of evacuation and flushing with argon. After incubation, the microplate was removed from the glovebox and fluorescence anisotropy was immediately measured. Interestingly, binding of BODIPY-AG to Hsp90 results in simultaneous increases in fluorescence anisotropy (FA) and intensity, whereas binding to Grp94 gives relatively little change in fluorescence intensity. Triplicate data points were collected for each binding or competition curve. Competition binding curves were fitted by a four-parameter logistic function:

$$FA = FA_{\min} + \frac{(FA_{\max} - FA_{\min})}{1 + (\{EC_{50}\}/\{[E]_{\text{total}}\})^{\text{Hill coefficient}}}$$

Dissociation of 17-AAG from Hsp90 (Complex). The dissociation rate of **1b** from either purified human Hsp90 protein or Hsp90 complex in cell lysates was determined using a spin column assay. [Allylamino- 3H]-17-AAG (20 Ci/mmol, $\geq 97\%$ pure by HPLC) was purchased from Moravsek Biochemicals (Brea, CA). 200 μ Ci (10 nmol) of [3H]-17-AAG in ethanol was dried under vacuum and mixed with 30 nmole of unlabeled **1b** in DMSO to give a stock solution of 1 mM [3H]-17-AAG with a SA of 3×10^6 – 4×10^6 cpm/nmol. The binding reaction contained 400 nM Hsp90, 4.0 μ M [3H]-17-AAG, and 0.38 mg/mL BGG in assay buffer (20 mM HEPES–KOH, pH 7.3, 1.0 mM EDTA, 100 mM KCl, 5.0 mM $MgCl_2$, 0.01% NP-40, 1.0 mM *fresh* DTT, and Complete protease inhibitor). Bovine γ -globulin was included as carrier protein for purified Hsp90 protein only. Alternatively, cell lysates (prepared as described in Kamal et al.²⁰) from normal human dermal fibroblasts (NHDF, 5.0 mg/mL total protein) or the breast cancer cell line SKBR3 (1.5 mg/mL) were used in place of purified Hsp90 protein. After ≥ 2 h incubation at 37 °C, 65 μ L of the binding

reaction was passed sequentially through two Zeba desalting spin columns (Pierce Biotechnology, Rockford, IL) to remove unbound ligand. In the dissociation reaction (650 μ L), the desalted protein solution containing bound [3 H]-17-AAG was diluted with unlabeled **1b** to give final concentrations of \sim 40 nM Hsp90, 40 μ M 17-AAG, and 0.48 mg/mL BGG in assay buffer. Similarly, the desalted cell lysates were diluted 10-fold with **1b** at 20 μ M final concentration. Unlabeled 17-AAG was present at \geq 1000-fold excess to Hsp90 to ensure that dissociation of [3 H]-17-AAG was practically irreversible. At various times of incubation (37 $^{\circ}$ C), 60 μ L of the dissociation reaction was withdrawn and passed sequentially through two Zeba spin columns. The flow-through fractions were analyzed on a MicroBeta microplate scintillation counter (Perkin-Elmer, Boston, MA). Dissociation kinetics was fitted with a single-exponential function $A = A_0 \times \exp^{-kt} + A_{\infty}$ to derive the first-order rate constant k .

Viability Assay. Human breast cancer cell line SKBR3 and ovarian cancer cell line SKOV3 were obtained from the American Type Culture Collection (Manassas, VA) and cultured in RPMI-1640 medium supplemented with 10% heat-inactivated FBS, 50 Units/mL streptomycin and 50 Units/mL penicillin at 37 $^{\circ}$ C in 5% CO₂. The cells were dissociated with 0.05% trypsin and 0.02% EDTA in phosphate-buffered saline without calcium and magnesium prior to plating for experimentation.

Viability studies were performed using the vital mitochondrial function stain Alamar Blue (Biosource International, Camarillo, CA). After cells were incubated in 96-well plates (200 μ L) in the presence or absence of compounds, 20 μ L of Alamar Blue solution was added and the plate was incubated for 4–6 h at 37 $^{\circ}$ C. The reduction of Alamar Blue signal was monitored by fluorescence at $\lambda_{\text{Ex}} = 544$ nm and $\lambda_{\text{Em}} = 590$ nm.

Her2 and Hsp70 Whole Cell Immunodetection. For whole cell immunodetection, 20 000 cells were plated into 96-well microtiter plates in 200 μ L of growth medium and allowed to attach to the plates overnight at 37 $^{\circ}$ C. Growth medium supplemented with compound or vehicle (DMSO or 75 mM citrate buffer, 75 mM ascorbate, pH 3.0–3.3) was added to the wells, and the plates were incubated again at 37 $^{\circ}$ C. Following different incubation times, the cells were washed twice with 70 μ L ice-cold Tris-buffered saline containing 0.1% Tween 20 (TBST) and the supernatant was aspirated. Ice-cold methanol (50 μ L) was then added to each well, and the plate was incubated at 4 $^{\circ}$ C for 10 min. Methanol was removed by washing with TBST (2 \times 100 μ L). The plates were further incubated with 100 μ L SuperBlock (Pierce Biotechnology, Rockford, IL) for 1 h at room temperature and overnight at 4 $^{\circ}$ C with the primary antibody (anti-Her2 or anti-Hsp70, Santa Cruz Biotechnology, Santa Cruz, CA) at a dilution of 1:200 in SuperBlock. Each well was washed with TBST (2 \times 100 μ L) and incubated at room temperature with horseradish peroxidase-linked secondary antibody (50 μ L, 1:1000 in SuperBlock, together with Hoechst reagent at 1:5000). After removal of unbound antibody by washing with TBST (2 \times 100 μ L), chemiluminescent substrate solution was added (20 μ L). After 5 min, plates were read by scanning each well for 0.1 s in the luminescence mode on an Envision microplate reader. Readings from wells where the primary antibody was omitted were used as background. The plates were then read in the fluorescence mode ($\lambda_{\text{Ex}} = 340$ nm and $\lambda_{\text{Em}} = 460$ nm). The relative fluorescence unit (RFU) values were used to normalize the relative luminescence unit (RLU) values to give luminescence intensity per number of cells. The ratio obtained from compound-treated cells versus vehicle-treated cells was plotted as a function of drug concentration to yield the EC₅₀ values.

Acknowledgment. We thank the project team at Infinity Pharmaceuticals, Inc., particularly Dr. Margaret Read, for their cooperation and support. We would also like to thank Prof. Matthew Shair of Harvard University for helpful discussions.

Supporting Information Available: Additional comments on analysis of data from Hsp90 binding assay. This material is available free of charge via the Internet at <http://pubs.acs.org>.

References

- Chiosis, G.; Vilenchik, M.; Kim, J.; Solit, D. Hsp90: the vulnerable chaperone. *Drug Discovery Today* **2004**, *9*, 881–888.
- Bagatell, R.; Whitesell, L. Altered Hsp90 function in cancer: a unique therapeutic opportunity. *Mol. Cancer Ther.* **2004**, *3*, 1021–1030.
- Workman, P. Combinatorial attack on multistep oncogenesis by inhibiting the Hsp90 molecular chaperone. *Cancer Lett* **2004**, *206*, 149–157.
- Sreedhar, A. S.; Soti, C.; Csermely, P. Inhibition of Hsp90: a new strategy for inhibiting protein kinases. *Biochim. Biophys. Acta* **2004**, *1697*, 233–242.
- Isaacs, J. S.; Xu, W.; Neckers, L. Heat shock protein 90 as a molecular target for cancer therapeutics. *Cancer Cell* **2003**, *3*, 213–217.
- Wegele, H.; Muller, L.; Buchner, J. Hsp70 and Hsp90-a relay team for protein folding. *Rev. Physiol. Biochem. Pharmacol.*, **2004**.
- Lai, B. T.; Chin, N. W.; Stanek, A. E.; Keh, W.; Lanks, K. W. Quantitation and intracellular localization of the 85K heat shock protein by using monoclonal and polyclonal antibodies. *Mol. Cell Biol.* **1984**, *4*, 2802–2810.
- Becker, B.; Multhoff, G.; Farkas, B.; Wild, P. J.; Landthaler, M. et al. Induction of Hsp90 protein expression in malignant melanomas and melanoma metastases. *Exp. Dermatol.* **2004**, *13*, 27–32.
- Lim, S. O.; Park, S. J.; Kim, W.; Park, S. G.; Kim, H. J. et al. Proteomic analysis of hepatocellular carcinoma. *Biochem. Biophys. Res. Commun.* **2002**, *291*, 1031–1037.
- Vercoutter-Edouart, A. S.; Czeszak, X.; Crepin, M.; Lemoine, J.; Boilly, B. et al. Proteomic detection of changes in protein synthesis induced by fibroblast growth factor-2 in MCF-7 human breast cancer cells. *Exp. Cell Res.* **2001**, *262*, 59–68.
- Ogata, M.; Naito, Z.; Tanaka, S.; Moriyama, Y.; Asano, G. Overexpression and localization of heat shock proteins mRNA in pancreatic carcinoma. *J. Nippon Med. Sch.* **2000**, *67*, 177–185.
- Cardillo, M. R.; Sale, P.; Di Silverio, F. Heat shock protein-90, IL-6 and IL-10 in bladder cancer. *Anticancer Res.* **2000**, *20*, 4579–4583.
- Ferrarini, M.; Heltai, S.; Zocchi, M. R.; Rugarli, C. Unusual expression and localization of heat-shock proteins in human tumor cells. *Int. J. Cancer* **1992**, *51*, 613–619.
- Jameel, A.; Skilton, R. A.; Campbell, T. A.; Chander, S. K.; Coombes, R. C. et al. Clinical and biological significance of HSP89 alpha in human breast cancer. *Int. J. Cancer* **1992**, *50*, 409–415.
- Chant, I. D.; Rose, P. E.; Morris, A. G. Analysis of heat-shock protein expression in myeloid leukaemia cells by flow cytometry. *Br. J. Haematol.* **1995**, *90*, 163–168.
- Yufu, Y.; Nishimura, J.; Nawata, H. High constitutive expression of heat shock protein 90 alpha in human acute leukemia cells. *Leuk. Res.* **1992**, *16*, 597–605.
- Gorre, M. E.; Ellwood-Yen, K.; Chiosis, G.; Rosen, N.; Sawyers, C. L. BCR-ABL point mutants isolated from patients with imatinib mesylate-resistant chronic myeloid leukemia remain sensitive to inhibitors of the BCR-ABL chaperone heat shock protein 90. *Blood* **2002**, *100*, 3041–3044.
- Shimamura, T.; Lowell, A. M.; Engelman, J. A.; Shapiro, G. I. Epidermal growth factor receptors harboring kinase domain mutations associate with the heat shock protein 90 chaperone and are destabilized following exposure to geldanamycins. *Cancer Res.* **2005**, *65*, 6401–6408.
- Vilenchik, M.; Solit, D.; Basso, A.; Huez, H.; Lucas, B. et al. Targeting wide-range oncogenic transformation via PU24FCL, a specific inhibitor of tumor Hsp90. *Chem. Biol.* **2004**, *11*, 787–797.
- Kamal, A.; Thao, L.; Sensintaffar, J.; Zhang, L.; Boehm, M. F. et al. A high-affinity conformation of Hsp90 confers tumour selectivity on Hsp90 inhibitors. *Nature* **2003**, *425*, 407–410.
- Chiosis, G.; Huez, H.; Rosen, N.; Mimnaugh, E.; Whitesell, L. et al. 17AAG: low target binding affinity and potent cell activity—finding an explanation. *Mol. Cancer Ther.* **2003**, *2*, 123–129.
- Janin, Y. L. Heat shock protein 90 inhibitors. A text book example of medicinal chemistry? *J. Med. Chem.* **2005**, *48*, 7503–7512.
- Fujiwara, H.; Yamakuni, T.; Ueno, M.; Ishizuka, M.; Shinkawa, T. et al. IC101 induces apoptosis by Akt dephosphorylation via an inhibition of heat shock protein 90-ATP binding activity accompanied by preventing the interaction with Akt in L1210 cells. *J. Pharmacol. Exp. Ther.* **2004**, *310*, 1288–1295.
- Banerji, U.; O'Donnell, A.; Scurr, M.; Pacey, S.; Stapleton, S. et al. Phase I pharmacokinetic and pharmacodynamic study of 17-allyl-amino, 17-demethoxygeldanamycin in patients with advanced malignancies. *J. Clin. Oncol.* **2005**, *23*, 4152–4161.
- Solit, D. B.; Egorin, M.; Kopil, C.; Delacruz, A.; Shaffer, D. et al. Phase I Pharmacokinetic and Pharmacodynamic trial of docetaxel and 17AAG (17-allylamino-17-demethoxygeldanamycin). *J. Clin. Oncol. (ASCO Meeting Abstr.)* **2005**, *23*, 3051.

- (26) Chanan-Khan, A.; Alsina, M.; Carroll, M.; Landrigan, B.; Doss, D. et al. Dose escalating trial of 17-AAG with bortezomib (BZ) in patients with relapsed refractory multiple myeloma (MM). *J. Clin. Oncol. (ASCO Meeting Abstr.)* **2005**, *23*, 6682.
- (27) Mitsiades, C.; Chanan-Khan, A.; Alsina, M.; Doss, D.; Landrigan, B. et al. Phase I trial of 17-AAG in patients with relapsed and refractory multiple myeloma (MM). *J. Clin. Oncol. (ASCO Meeting Abstr.)* **2005**, *23*, 3056.
- (28) Jez, J. M.; Chen, J. C.; Rastelli, G.; Stroud, R. M.; Santi, D. V. Crystal Structure and Molecular Modeling of 17-DMAG in Complex with Human Hsp90. *Chem. Biol.* **2003**, *10*, 361–368.
- (29) Roe, S. M.; Prodromou, C.; O'Brien, R.; Ladbury, J. E.; Piper, P. W. et al. Structural basis for inhibition of the Hsp90 molecular chaperone by the antitumor antibiotics radicicol and geldanamycin. *J. Med. Chem.* **1999**, *42*, 260–266.
- (30) Stebbins, C. E.; Russo, A. A.; Schneider, C.; Rosen, N.; Hartl, F. U. et al. Crystal structure of an Hsp90-geldanamycin complex: targeting of a protein chaperone by an antitumor agent. *Cell* **1997**, *89*, 239–250.
- (31) Nimmanapalli, R.; O'Bryan, E.; Bhalla, K. Geldanamycin and its analogue 17-allylamino-17-demethoxygeldanamycin lowers Bcr-Abl levels and induces apoptosis and differentiation of Bcr-Abl-positive human leukemic blasts. *Cancer Res.* **2001**, *61*, 1799–1804.
- (32) An, W. G.; Schulte, T. W.; Neckers, L. M. The heat shock protein 90 antagonist geldanamycin alters chaperone association with p210bcr-abl and v-src proteins before their degradation by the proteasome. *Cell Growth Differ.* **2000**, *11*, 355–360.
- (33) Whitesell, L.; Sutphin, P.; An, W. G.; Schulte, T.; Blagosklonny, M. V. et al. Geldanamycin-stimulated destabilization of mutated p53 is mediated by the proteasome in vivo. *Oncogene* **1997**, *14*, 2809–2816.
- (34) Schulte, T. W.; An, W. G.; Neckers, L. M. Geldanamycin-induced destabilization of Raf-1 involves the proteasome. *Biochem. Biophys. Res. Commun.* **1997**, *239*, 655–659.
- (35) Sydor, J. R.; Normant, E.; Pien, C. S.; Porter, J.; Ge, J. et al. Development of IPI-504, a novel anti-cancer agent directed against Hsp90. Manuscript submitted.
- (36) Schnur, R. C.; Corman, M. L.; Gallaschun, R. J.; Cooper, B. A.; Dee, M. F. et al. Inhibition of the oncogene product p185erbB-2 in vitro and in vivo by geldanamycin and dihydrogeldanamycin derivatives. *J. Med. Chem.* **1995**, *38*, 3806–3812.
- (37) Schnur, R. C.; Corman, M. L.; Gallaschun, R. J.; Cooper, B. A.; Dee, M. F. et al. erbB-2 oncogene inhibition by geldanamycin derivatives: synthesis, mechanism of action, and structure–activity relationships. *J. Med. Chem.* **1995**, *38*, 3813–3820.
- (38) Egorin, M. J.; Rosen, D. M.; Wolff, J. H.; Callery, P. S.; Musser, S. M. et al. Metabolism of 17-(allylamino)-17-demethoxygeldanamycin (NSC 330507) by murine and human hepatic preparations. *Cancer Res.* **1998**, *58*, 2385–2396.
- (39) Le Brazidec, J. Y.; Kamal, A.; Busch, D.; Thao, L.; Zhang, L. et al. Synthesis and biological evaluation of a new class of geldanamycin derivatives as potent inhibitors of Hsp90. *J. Med. Chem.* **2004**, *47*, 3865–3873.
- (40) Guo, W.; Reigan, P.; Siegel, D.; Zirrolli, J.; Gustafson, D. et al. Formation of 17-allylamino-demethoxygeldanamycin (17-AAG) hydroquinone by NAD(P)H: quinone oxidoreductase 1: role of 17-AAG hydroquinone in heat shock protein 90 inhibition. *Cancer Res.* **2005**, *65*, 10006–10015.
- (41) Unidentified acylated products were not fully characterized.
- (42) Kim, J.; Felts, S.; Llauger, L.; He, H.; Huez, H. et al. Development of a fluorescence polarization assay for the molecular chaperone Hsp90. *J. Biomol. Screen* **2004**, *9*, 375–381.
- (43) Llauger-Bufi, L.; Felts, S. J.; Huez, H.; Rosen, N.; Chiosis, G. Synthesis of novel fluorescent probes for the molecular chaperone Hsp90. *Bioorg. Med. Chem. Lett.* **2003**, *13*, 3975–3978.
- (44) Carreras, C. W.; Schirmer, A.; Zhong, Z.; Santi, D. V. Filter binding assay for the geldanamycin-heat shock protein 90 interaction. *Anal. Biochem.* **2003**, *317*, 40–46.
- (45) McLaughlin, S. H.; Ventouras, L. A.; Lobbezoo, B.; Jackson, S. E. Independent ATPase activity of Hsp90 subunits creates a flexible assembly platform. *J. Mol. Biol.* **2004**, *344*, 813–826.
- (46) Prodromou, C.; Roe, S. M.; O'Brien, R.; Ladbury, J. E.; Piper, P. W. et al. Identification and structural characterization of the ATP/ADP-binding site in the Hsp90 molecular chaperone. *Cell* **1997**, *90*, 65–75.
- (47) Rosser, M. F.; Nicchitta, C. V. Ligand interactions in the adenosine nucleotide-binding domain of the Hsp90 chaperone, GRP94. I. Evidence for allosteric regulation of ligand binding. *J. Biol. Chem.* **2000**, *275*, 22798–22805.
- (48) Munster, P. N.; Marchion, D. C.; Basso, A. D.; Rosen, N. Degradation of HER2 by ansamycins induces growth arrest and apoptosis in cells with HER2 overexpression via a HER3, phosphatidylinositol 3'-kinase-AKT-dependent pathway. *Cancer Res.* **2002**, *62*, 3132–3137.
- (49) Whitesell, L.; Mimnaugh, E. G.; De Costa, B.; Myers, C. E.; Neckers, L. M. Inhibition of heat shock protein HSP90-pp60v-src heteroprotein complex formation by benzoquinone ansamycins: essential role for stress proteins in oncogenic transformation. *Proc. Natl. Acad. Sci. U.S.A.* **1994**, *91*, 8324–8328.
- (50) Wang, M.; Shen, G.; Blagg, B. S. Radanamycin, a macrocyclic chimera of radicicol and geldanamycin. *Bioorg. Med. Chem. Lett.* **2006**.
- (51) Patel, K.; Piagentini, M.; Rascher, A.; Tian, Z. Q.; Buchanan, G. O. et al. Engineered biosynthesis of geldanamycin analogs for Hsp90 inhibition. *Chem. Biol.* **2004**, *11*, 1625–1633.
- (52) Muroi, M.; Izawa, M.; Kosai, Y.; Asai, M. Macbecins I and II, new antitumor antibiotics. II. Isolation and characterization. *J. Antibiot. (Tokyo)* **1980**, *33*, 205–212.
- (53) Lee, Y. S.; Marcu, M. G.; Neckers, L. Quantum chemical calculations and mutational analysis suggest heat shock protein 90 catalyzes trans-cis isomerization of geldanamycin. *Chem. Biol.* **2004**, *11*, 991–998.
- (54) Neckers, L.; Lee, Y. S. Cancer: the rules of attraction. *Nature* **2003**, *425*, 357–359.
- (55) Dymock, B. W.; Barril, X.; Brough, P. A.; Cansfield, J. E.; Massey, A. et al. Novel, Potent Small-Molecule Inhibitors of the Molecular Chaperone Hsp90 Discovered through Structure-Based Design. *J. Med. Chem.* **2005**, *48*, 4212–4215.
- (56) Tian, Z. Q.; Liu, Y.; Zhang, D.; Wang, Z.; Dong, S. D. et al. Synthesis and biological activities of novel 17-aminogeldanamycin derivatives. *Bioorg. Med. Chem.* **2004**, *12*, 5317–5329.
- (57) Chiosis, G.; Timaul, M. N.; Lucas, B.; Munster, P. N.; Zheng, F. F. et al. A small molecule designed to bind to the adenine nucleotide pocket of Hsp90 causes Her2 degradation and the growth arrest and differentiation of breast cancer cells. *Chem. Biol.* **2001**, *8*, 289–299.
- (58) Sullivan, W.; Stensgard, B.; Caucutt, G.; Bartha, B.; McMahon, N. et al. Nucleotides and two functional states of hsp90. *J. Biol. Chem.* **1997**, *272*, 8007–8012.
- (59) Dittmar, K. D.; Banach, M.; Galigniana, M. D.; Pratt, W. B. The role of DnaJ-like proteins in glucocorticoid receptor.hsp90 hetero-complex assembly by the reconstituted hsp90.p60.hsp70-foldsosome complex. *J. Biol. Chem.* **1998**, *273*, 7358–7366.
- (60) Dollins, D. E.; Immormino, R. M.; Gewirth, D. T. Structure of unliganded GRP94, the ER Hsp90: Basis for nucleotide-induced conformational change. *J. Biol. Chem.* **2005**.
- (61) Immormino, R. M.; Dollins, D. E.; Shaffer, P. L.; Soldano, K. L.; Walker, M. A. et al. Ligand-induced conformational shift in the N-terminal domain of GRP94, an Hsp90 chaperone. *J. Biol. Chem.* **2004**, *279*, 46162–46171.
- (62) Soldano, K. L.; Jivan, A.; Nicchitta, C. V.; Gewirth, D. T. Structure of the N-terminal domain of GRP94. Basis for ligand specificity and regulation. *J. Biol. Chem.* **2003**, *278*, 48330–48338.
- (63) Randow, F.; Seed, B. Endoplasmic reticulum chaperone gp96 is required for innate immunity but not cell viability. *Nat. Cell Biol.* **2001**, *3*, 891–896.
- (64) Jagannath, S.; Siegel, D.; Richardson, P.; Mazumder, A.; Sydor, J. et al. Phase I Clinical Trial of IPI-504, a novel, water-soluble Hsp90 inhibitor, in patients with relapsed/refractory multiple myeloma (MM). *Blood* **2005**, *106*, [Abstract #2560].
- (65) Sasaki, K.; Inoue, Y. Geldanamycin Derivatives and Antitumor Drug. U.S. Patent 4,261, 989, 1981.
- (66) Snader, K. M.; Vishnuvajjala, B. R.; Hollingshead, M. G.; Sausville, E. A. Geldanamycin Derivative and Method of Treating Cancer Using Same. PCT Patent Application WO 02/079167, 2002.
- (67) Zhang, L.; Boehm, M. F.; Zegar, S. Process for Preparing 17-Allyl Amino Geldanamycin (17-AAG) and Other Ansamycins. PCT Patent Application WO 03/026571 A2, 2003.
- (68) Abbreviations: 17-AAG, 17-Allylamino-17-demethoxygeldanamycin; 17-AG, 17-amino-17-demethoxygeldanamycin; 17-DMAG, 17-dimethylaminoethylamino-17-demethoxygeldanamycin; BGG, bovine γ -globulin; ADP, adenosine 5'-diphosphate; ATP, adenosine 5'-triphosphate; BODIPY, boron difluoride dipyrromethene; BODIPY-AG, BODIPY-labeled geldanamycin analogue; EGFR, epidermal growth factor receptor; ER, endoplasmic reticulum; ES⁺, electrospray positive; FA, fluorescence anisotropy; FP, fluorescence polarization; Grp94, the 94 kDa glucose regulated protein; HPLC, high-pressure liquid chromatography; HRMS, High-resolution mass spectra; HSF-1, heat shock factor-1; Hsp90, the 90 kDa heat shock protein; IR, infrared; NHDF, normal human dermal fibroblast; PVDF, polyvinylidene fluoride; RFU, relative fluorescence unit; RLU, relative luminescence unit; $t_{1/2}$, half-life; TBST, Tris-buffered saline containing 0.1% Tween 20; TLR, Toll-like receptors; Trap1, tumor necrosis factor receptor-associated protein 1.